Proceedings of the ASME 2012 International Mechanical Engineering Congress & Exposition
IMECE2012
November 9-15, 2012, Houston, Texas, USA

IMECE2012-87672

A POLYMER-BASED MICROFLUIDIC RESISTIVE SENSOR FOR DETECTING DISTRIBUTED LOADS

Wenting Gu[1], Peng Cheng[1], Arindam Ghosh[1], Yuxi Liao[2,3], Boxiong Liao[3], Ali Beskok[1], Zhili Hao[1]
[1]Department of Mechanical and Aerospace Engineering, Old Dominion University
Norfolk, VA USA
[2]School of Electrical and Computer Engineering, Georgia Institute of Technology
Atlanta, GA, USA
[3]Precision Sensors and Systems, LLC, Virginia Beach, VA USA

ABSTRACT

This paper reports on a polymer-based microfluidic resistive sensor for detecting distributed loads. The sensor is comprised of a polymer rectangular microstructure with an embedded electrolyte-filled microchannel and an array of electrodes aligned along the microchannel length. Electrolyte solution in the microchannel serves as impedance transduction. Distributed loads acting on the polymer microstructure give rise to different deflection along the microstructure length, which is recorded as the resistance change in electrolyte solution. This sensor can detect distributed loads by monitoring the resistance change at each pair of electrodes. A sensor with an in-plane dimension of ~20mm×10mm and five pairs of electrodes is fabricated using a CNC machine. 1M KCl solution is used as the electrolyte. Using a custom built electronic circuit on breadboard and a custom LabVIEW program, the static and dynamic performance of the sensor is characterized, demonstrating the feasibility of employing this sensor to detect distributed loads.

1 INTRODUCTION

Microfluidic devices have been widely explored for various biological and chemical applications [1]. Generally speaking, these microfluidic devices contain microchannels or microchambers where fluids and/or particles are manipulated and analyzed. Owing to its low cost and biocompatibility, polydimethylsiloxane (PDMS) has become one of the most commonly used building material for microfluidic devices [2]. Standard fabrication technologies, including forming a patterned PDMS structure and bonding a PDMS structure to a glass substrate, has been well established for fabricating PDMS-based microfluidic devices. In this paper, we demonstrate the use of a PDMS rectangular microstructure with an embedded electrolyte-filled microchannel for detecting distributed loads, which are commonly encountered in biomedical [3], robotics [4], food processing and manufacturing applications [5].

In the meantime, miniature tactile sensors, employing different transduction mechanisms and fabricated using various fabrication technologies, have been developed for biomedical and robotics applications [6, 7], such as minimally invasive surgeries, tissue health diagnostics, and robotic fingertips. A general trend in the tactile sensing technology has been shifting the structural material from silicon to various polymers [8-13], due to their low elastic strength, which is compatible with a wide range of soft biological and viscoelastic materials, biocompatibility and removal of the need for protective packaging. Among these polymer-based tactile sensors, a few of them are essentially microfluidic devices in the sense that these devices contain a polymer microstructure filled with electrolyte. For instance, Gutierrez et al. [11] developed a parylene force sensor containing a parylene microchamber filled with an electrolyte. Tseng et al. [12] demonstrated a PDMS/polyimide tactile sensor including a hemispheric microchamber filled with an electrolyte and an initially empty microchannel. Park et al. [13] developed a PDMS tactile sensor encompassing a PDMS microchannel filled with eGaIn.

The core of the above mentioned microfluidic tactile sensors is a polymer microstructure filled with electrolyte. In response to an external load, the microstructure generates a deflection, and, as impedance transducer, electrolyte in the microstructure converts the deflection to an impedance

change. In terms of long-term stability, repeatability, and response time, the feasibility of employing electrolyte-filled polymer microstructures as tactile/force sensors has been demonstrated by these microfluidic sensors. However, the parylene-based force sensor [11] involves great fabrication complexity, and its electrolyte filling method renders it unsuitable for operation in dry environment. Although the fabrication of the PDMS/polyimide microfluidic device [12] is relatively simple, electrolyte filling and device operation is complex. In contrast, the PDMS tactile sensor [13] demonstrates great fabrication simplicity and ease of electrolyte filling. However, since the electrolyte in the whole PDMS microchannel is utilized for impedance transduction with the ends of the microchannel for electrical connection, this sensor is not capable of measuring distributed loads along the microchannel length.

In many practical applications, it is necessary to detect non-uniform distributed loads in aqueous and dry environments, which are induced by heterogeneous biological or viscoelastic materials or by texture of an object. For instance, Ahmadi et al. [3] demonstrated an optical fiber tactile sensor for detecting heterogeneous tissues in minimally invasive robotic surgery. In this tactile sensor, several fibers are embedded underneath a beam in order to convert the deflections at different locations along the beam into optical signals. Since this sensor is manually assembled together, it has the drawback of large dimension and high cost. In order to detect the texture of an object, a sensor array with high spatial resolution (1mm) is needed for a robotic fingertip [3, 6].

In this paper, we report the design, fabrication, and performance characterization of a PDMS-based microfluidic resistive sensor for detecting distributed loads. This sensor is comprised of a PDMS rectangular microstructure with an embedded electrolyte-filled microchannel and an array of electrodes allocated along the microstructure length. A prototype sensor is fabricated using a CNC machine. Electrolyte is filled into the sensor through the reservoirs at its ends. With a custom built electronic circuit and a custom LabVIEW program, the static and dynamic performance of the fabricated sensor is characterized, verifying the design concept of this sensor. As compared with the above mentioned polymer-based microfluidic tactile sensors, the sensor presented in this paper not only provides the capability of detecting distributed loads, but also offers quite a few advantages, including great fabrication simplicity, ease of electrolyte filling, and operation in both aqueous and dry environments.

2 DEVICE DESIGN AND OPERATION

Fig. 1 shows a schematic view of the PDMS-based microfluidic resistive sensor for detecting distributed loads. This sensor is comprised of a PDMS rectangular structure with an embedded electrolyte-filled microchannel and five pairs of metal electrodes. Two reservoirs at the ends of the microstructure are utilized to fill the microchannel with an electrolyte and provide a conduit for electrolyte in the microchannel to flow in/out during the sensor operation. Each electrode pair has opposing electrodes along the channel width, and they record a change of electrical resistance across them. Five pairs of electrodes are allocated along the microchannel length in order to detect the distributed loads acting on the microstructure surface. A rectangular microstructure design is chosen here for simplicity. Certainly, other structural geometries can be easily realized given that the sensor design is compatible with the fabrication process as described later on. Selection of PDMS as the building material for the rectangular microstructure offers great fabrication simplicity and biocompatibility.

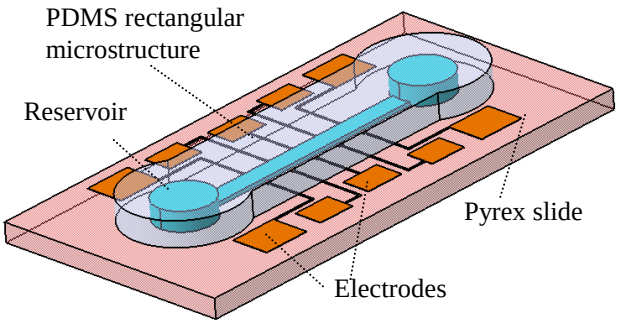

Fig. 1: Schematic view of the PDMS-based microfluidic resistive sensor consisting of a PDMS rectangular structure with an embedded electrolyte-filled microchannel and five pairs of electrodes allocated along the microstructure length.

The electrical equivalent circuit across each pair of electrodes of the sensor is depicted in Fig. 2. Electrolyte across the electrodes can be simplified as a resistor, R_s, and a capacitor, C_s, in parallel. Owing to the electrical double layer formed at the interface between an electrode and electrolyte, each electrolyte-electrode interface is treated as a double layer capacitor, C_{dl}, and a charge transfer resistor, R_{ct}, in series [12]. Therefore, the impedance across the two electrodes is written as:

$$Z = 2Z_{DL} + \frac{R_S}{1 + j\omega C_S R_S} \quad (1)$$

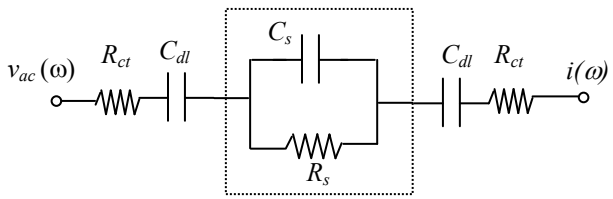

Fig. 2: Equivalent electrical circuit across the two electrodes of the PDMS-based microfluidic resistive tactile sensor

where Z_{DL} denotes the impedance of each electrolyte-electrolyte interface, and ω denotes the frequency of the ac voltage signal, $v_{ac}(\omega)$, which is applied to one electrode during operation. By choosing an appropriate electrolyte and the operation frequency of the ac voltage signal, the impedance of the electrolyte-electrode interfaces and the capacitance across the electrode pair can be neglected. Then, the sensor can be treated solely as a resistor. It should be pointed out that, rather

Table 1 Key design parameters and their values of the PDMS-based microfluidic resistive sensor

Design parameter	Value	Symbol
Length of the electrolyte-filled microchannel	12mm	L_m
Width of the electrolyte-filled microchannel	1mm	W_{m1}
Height of the electrolyte-filled microchannel	200μm	h_{m1}
Length of the PDMS rectangular microstructure	12mm	L_m
Width of the PDMS rectangular microstructure	5mm	W_{m2}
Height of the top of the PDMS rectangular microstructure	1.0mm	h_{m2}
Distance between neighboring pairs of electrodes	1.5mm	X_E
Distance between each pair of electrodes	600μm	D_E

than capacitive sensing, resistive sensing is chosen in order to eliminate the interference from its working environment [6].

Fig. 3 illustrates the operation principle of the sensor, together with the key design parameters of this sensor being symbolized. The key design parameters and their values of the device are summarized in Table 1. Distributed loads acting on the device surface deflect the compliant PDMS microstructure at different levels along the microstructure length and compress partial electrolyte into the reservoirs. Consequently, the cross section of the resistor formed by electrolyte across each pair of electrodes is reduced and this reduced cross section registers as a resistance change. The resistance change across each pair of electrodes is related to its cross section by:

$$R_i = \frac{\rho_E \cdot D_E}{A_E(z_i)} \tag{2}$$

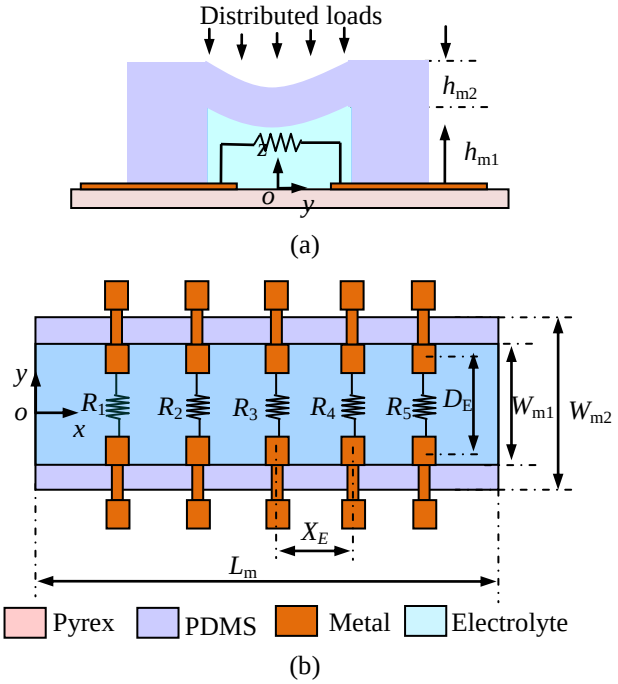

Fig. 3: (a) Side view and (b) top view of the PDMS-based microfluidic resistive sensor (drawn not to scale for better illustration)

where ρ_E is the electrical conductivity of electrolyte; D_E is the distance across the two electrodes; A_E is the microchannel cross-section, which is a function of the deflection, z_i, of the top of the microstructure; and Subscript i denotes the parameters associated with the i^{th} pair of electrodes. By measuring the resistance change at the five pairs of electrodes along the microstructure length, distributed loads acting on the device surface can be obtained.

Subjected to distributed loads, electrolyte in the microchannel flows into the reservoirs, since electrolyte in the sensor is incompressible. Thus, adding the reservoirs not only completely confines electrolyte within the sensor, but also allows electrolyte to freely flow during operation. This device can be operated in either aqueous or air environment, since electrolyte is confined within the device and the building materials of the device are nonconductive, except that the portion of the electrodes outside the PDMS microstructure needs to be covered with an insulating layer for operation in aqueous environment.

3 FABRICATION PROCESS

Fig. 4 shows the fabrication process for the PDMS-based microfluidic resistive sensor. First, 100nm/10nm-thick Au/Cr electrodes are deposited and patterned on one side of a 1mm-thick Pyrex slide. Then, a mold is made from polycarbonate using a CNC machine. The height of the mold determines the total height of the PDMS microstructure. The inverse of the microchannel and the reservoirs is patterned at the bottom of the mold. A 10:1 ratio of PDMS elastomer to curing agent (Sylgard 184kit, Dow Corning Corp.) is poured over the mold and cured to form the PDMS rectangular microstructure. Since the thickness of the PDMS layer above the mold plays a critical role in determining its sensitivity to distributed loads, this parameter can be controlled by varying the amount of PDMS poured into the mold. The cured PDMS structure is peeled off from the mold. The Pyrex slide with patterned electrode and the PDMS microstructure are treated with oxygen plasma and bonded together. Finally, a hole is punched into each reservoir and the microchannel is filled with1M KCl electrolyte solution using a syringe. Holes in the reservoirs can be further sealed or connected to a tube to avoid leakage.

Fig. 5 shows a couple of pictures of the fabricated device. One device is filled with colored solution for showing the dimension of the embedded microchannel. The other fabricated device is with filled KCl electrolyte and sealed with

two pieces of PDMS, and wires are bonded to the electrodes outside the PDMS microstructure for electrical connection. The microchannel has a dimension of 12mm×1mm×200μm. The distance between the centers of the two reservoirs is 15mm and the width of the PDMS rectangular microstructure is 5mm.

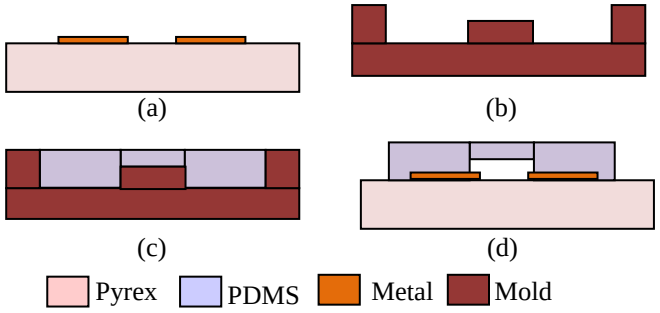

Fig. 4: Fabrication process of the polymer-based microfluidic resistive sensor (a) deposit and pattern Au/Cr electrode on a Pyrex slide (b) fabricate a mold for molding the PDMS microstructure (c) form the PDMS microstructure using the mold and (d) bond the PDMS microstructure to the patterned Pyrex slide

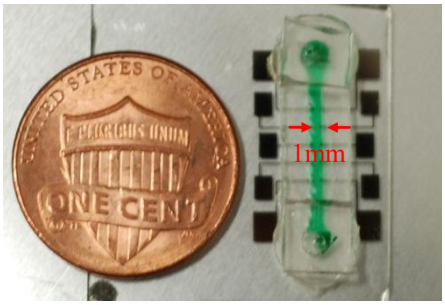

(a)

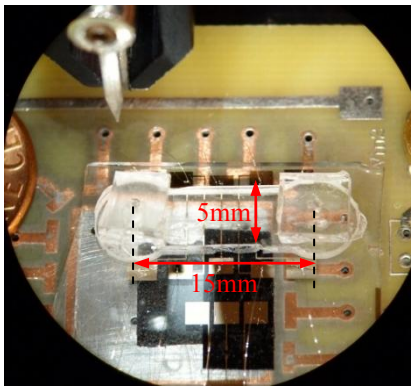

(b)

Fig. 5: Pictures of the fabricated sensors (a) filled with colored liquid showing the dimension of the embedded microchannel and (b) filled with KCl electrolyte and bonded with wires for electrical connection

4 PERFORMANCE CHARACTERIZATION

4.1 Electronic circuit

To test the fabricated device, a custom electronic circuit is designed and implemented on breadboard for measuring the resistance across a pair of electrodes, when the device is subjected to external loading. As shown in Fig. 6, the circuit for detecting the resistance across a pair of electrodes contains a transimpedance amplifier and a demodulation stage. An ac voltage signal, $v_{ac}(\omega)$, is applied to one electrode, while the current, $i(\omega)$, coming out from the other electrode, feeds in the inverting terminal of the OP-AMP (OPA656U). The sensing electrode is maintained at virtual ground by connecting the non-inverting terminal to the ground in order to minimize the effect of parasitics on this current signal. For simplicity, the output, v_1, of the transimpedance amplifier serves as two identical inputs for the multiplier (AD835) to avoid phase difference between the two inputs. The DC component, V_{out}, of the voltage output, v_2, of the multiplier, passes the following third order low-pass filter (LPF) and gives rise to the measurement of the resistance across the electrode pair. As shown in Fig. 7, this circuit is implemented on breadboard and can monitor the resistance across a pair of electrodes at a given time. To monitor all the five pairs of electrodes simultaneously, five similar electronic circuits and five ac signals are needed. The time constant of this circuit is simulated to be 11.6ms, as shown in Fig. 8.

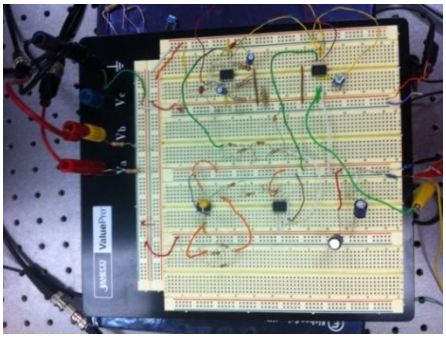

Fig. 7: A picture of the custom electronic circuit on breadboard

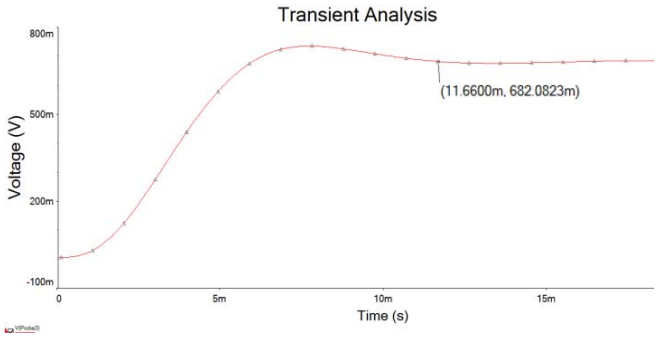

Fig. 8: Simulated time constant of the custom electronic circuit is 12ms

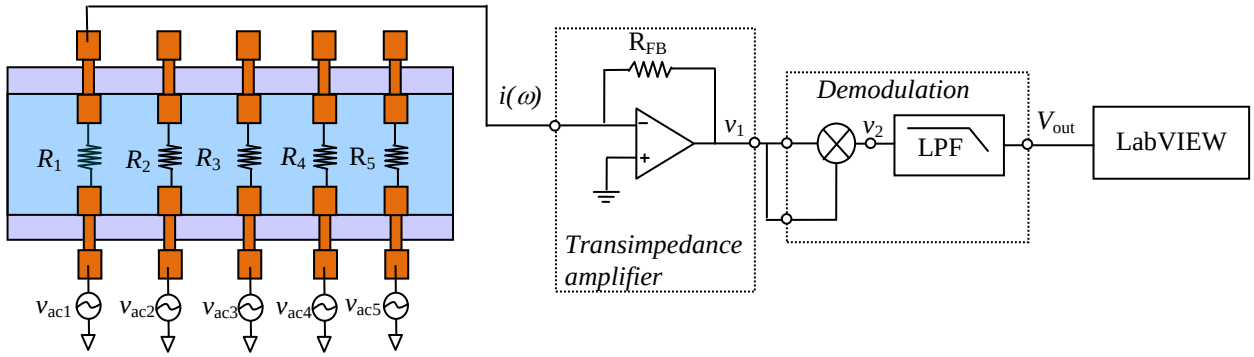

Fig. 6: Schematic of a custom electronic circuit connected to a pair of electrodes of the fabricated device for measuring the resistance across them

Now, we relate the DC voltage output of the electronic circuit to the resistance across a pair of electrodes of the sensor. Assume that the ac voltage signal is expressed as:

$$v_{ac} = \frac{1}{2} v_{PP} \cdot \sin(\omega t) \tag{3}$$

where v_{PP} and ω denote the peak-peak (p-p) value and the frequency of the ac voltage. Then, the current output from the device is given by:

$$i = \frac{v_{ac}}{R_i(z)} \tag{4}$$

The ac voltage output of the transimpedance amplifier is:

$$v_1(\omega) = \frac{v_{ac}}{R_i(z)} \cdot R_F \tag{5}$$

The DC voltage output of the demodulation stage is:

$$V_{out} = \frac{v_{PP}^2 \cdot R_F^2}{8 R_i^2(z)} \tag{6}$$

By using a few resistors with known values, the relation of the DC voltage output to the resistance from the electronic circuit is verified. Consequently, the resistance across a pair of electrodes of the sensor can be extracted from the measured DC voltage using the following relation:

$$R_i(z) = \frac{v_{PP} \cdot R_F}{2\sqrt{2V_{out}}} \tag{7}$$

The overall sensitivity of the sensor to the resistance becomes:

$$S = \frac{\partial V_{out}}{\partial R_i(z_i)} = -\frac{v_{PP}^2 \cdot R_F^2}{4 R_i^3(z_i)} \tag{8}$$

Hence, a large p-p value of the ac voltage and a large feedback resistance of the transimpedance amplifier contribute to a higher sensitivity of the sensor. Based on the initial resistance and the chosen operation frequency for the ac voltage signal, the resistance of the feedback resistor is fixed at R_F=970Ω. The p-p value of the ac voltage is varied to keep the DC voltage output around 0.12V when the sensor is not subjected to external loading, while keeping the OP-AMP and the multiplier working in their operation range.

4.2 Experimental setup and method

Fig. 9(a) shows the experimental setup for characterizing the performance of the PDMS-based microfluidic resistive sensor. A fabricated sensor is mounted on a PCB, where wires are bonded between electrodes of the sensor and copper electrodes on a PCB, as shown in Fig. 5. Then, the PCB is mounted on a custom fixture, which is further fixed on an optical table. A custom circular probe of 4mm in diameter is mounted on a micropositioner, as shown in Fig. 9(b). A controller associated with the micropositioner can precisely move the circular probe along the z-axis with a resolution of 0.2μm. Before each measurement, the circular probe is brought in contact with the PDMS rectangular microstructure surface, without deflecting the sensor. This is achieved by monitoring the change in resistance.

To measure the resistance across a pair of electrode, a function generator (HP33220A) is connected to one electrode for providing an ac voltage signal, while the other electrode is connected to the circuit on breadboard. The DC voltage output signal from the circuit is connected to PCI-6133 DAQ board, which feeds in a custom LabVIEW program for recording data every 0.1s for approximately 70sec. The recorded DC voltage output is then converted to resistance, according to Eq. (7). An important operation parameter is the frequency of the ac voltage. Care must be taken to ensure that this sensor is predominantly resistive so that any change in the measured DC voltage is solely caused by the resistance change across a pair of electrodes. Here, the frequency of the ac voltage signal is chosen to be 200kHz.

4.3 Experimental results

Dynamic performance

Using the controller associated with the micropostioner, a pre-defined deflection pattern, as shown in Fig. 10, is applied to deflect the sensor through the circular probe. The circular probe generates a deflection of 300μm in the sensor at a

constant speed of 300μm/s, remains at this deflection for 3s, and then goes back to the un-deflected position at the same constant speed. This deflection cycle repeats itself for roughly 70sec. The probe is aligned at different locations along the PDMS rectangular microstructure for deflecting the sensor with this pre-defined deflection pattern, and the DC voltage output is recorded across different pairs of electrodes, respectively. Due to the lack of enough equipment, the data is recorded for one pair of electrodes at a given time.

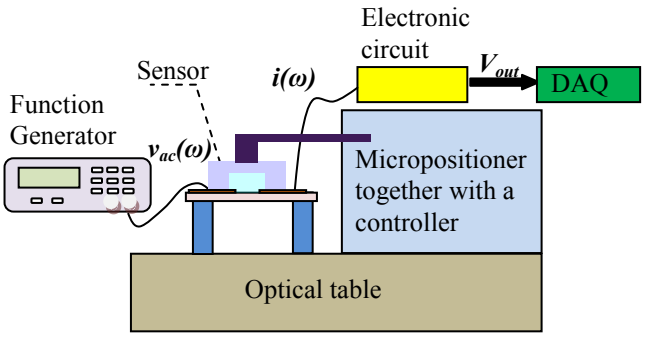

(a)

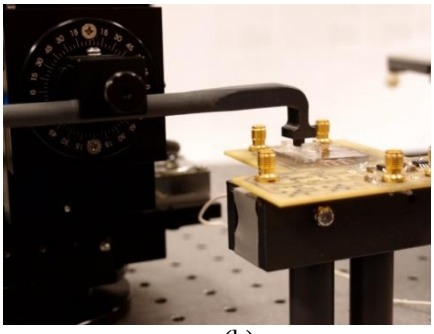

(b)

Fig. 9: (a) Schematic view of the experimental setup for testing the fabricated device and (b) picture of a custom circular probe mounted on a micropositioner, located above the fabricated sensor

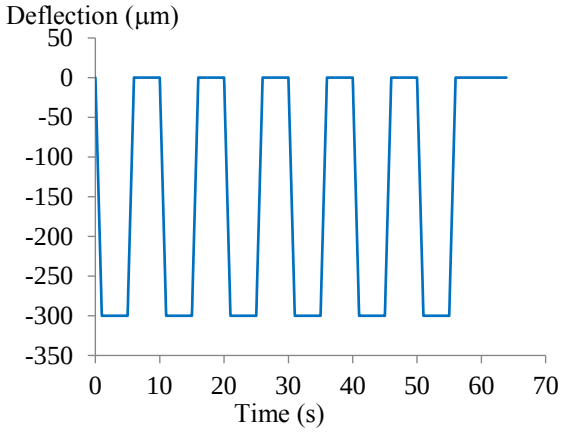

Fig. 10: Pre-defined deflection pattern of the circular probe

Fig 11 shows the measured data from the 1st pair of electrodes, when the circular probe is located at A and B, respectively, deflecting the sensor according to the pattern shown in Fig. 10. The ac voltage is kept at v_{pp}=1V and ω= 200kHz in this measurement. When this sensor is free of external loading, the resistance across this electrode pair is about 1020Ω, based on the DC output of 0.114V. When this sensor is deflected by 300μm at A, the DC output becomes 0.092V and thus the resistance increases to 1140Ω. The increase in resistance is caused by the cross section reduction of the electrolyte across this electrode pair. Similarly, when the sensor is deflected by 300μm at B, the DC output decreases to 0.88V and the resistance increases to 1160Ω. Since deflecting B causes more reduction in the cross section across this electrode pair than deflecting A, the resistance from deflecting B is higher than that from deflecting A.

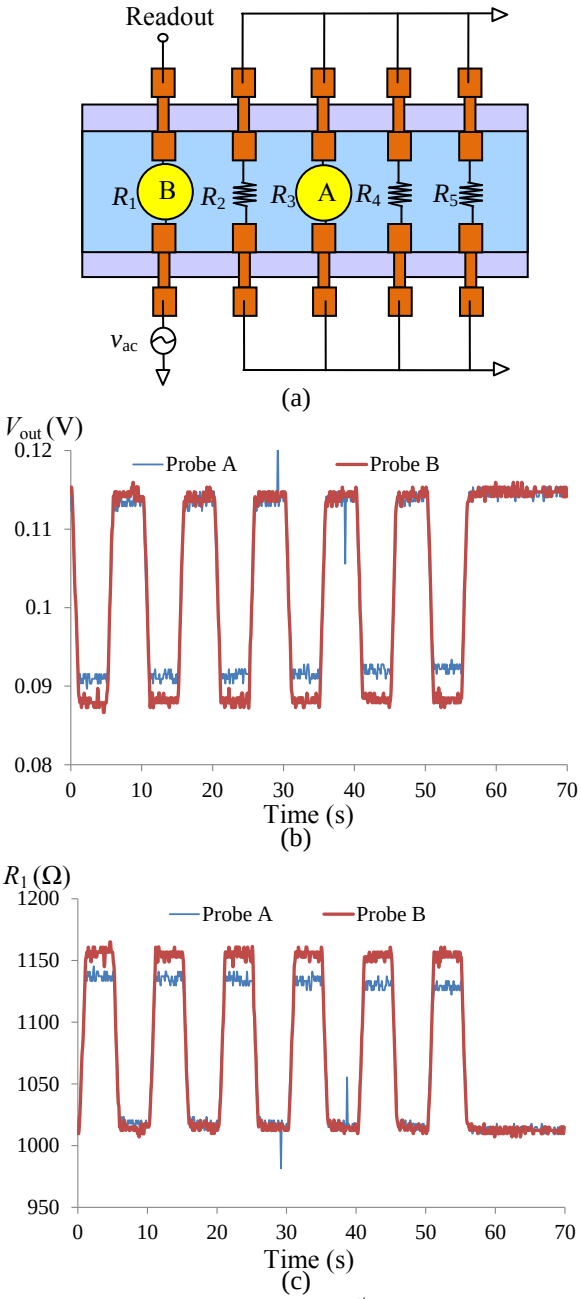

Fig. 11: Measured results from the 1st pair of electrodes, when the custom probe is located at A and B, respectively (v_{pp}=1V and ω= 200kHz) (a) locations of the probe (b) DC voltage output, and (c) resistance calculated from the DC voltage output

Fig. 12 shows the measured data from the 3rd pair of electrodes. The probe is utilized to deflect the sensor at A and B, respectively. The DC voltage is read out from the 3rd electrode pair. The ac voltage is maintained at v_{pp}=3V and ω= 200kHz in this measurement. Note that a high ac voltage is chosen in order to keep the original DC output around 0.12V.

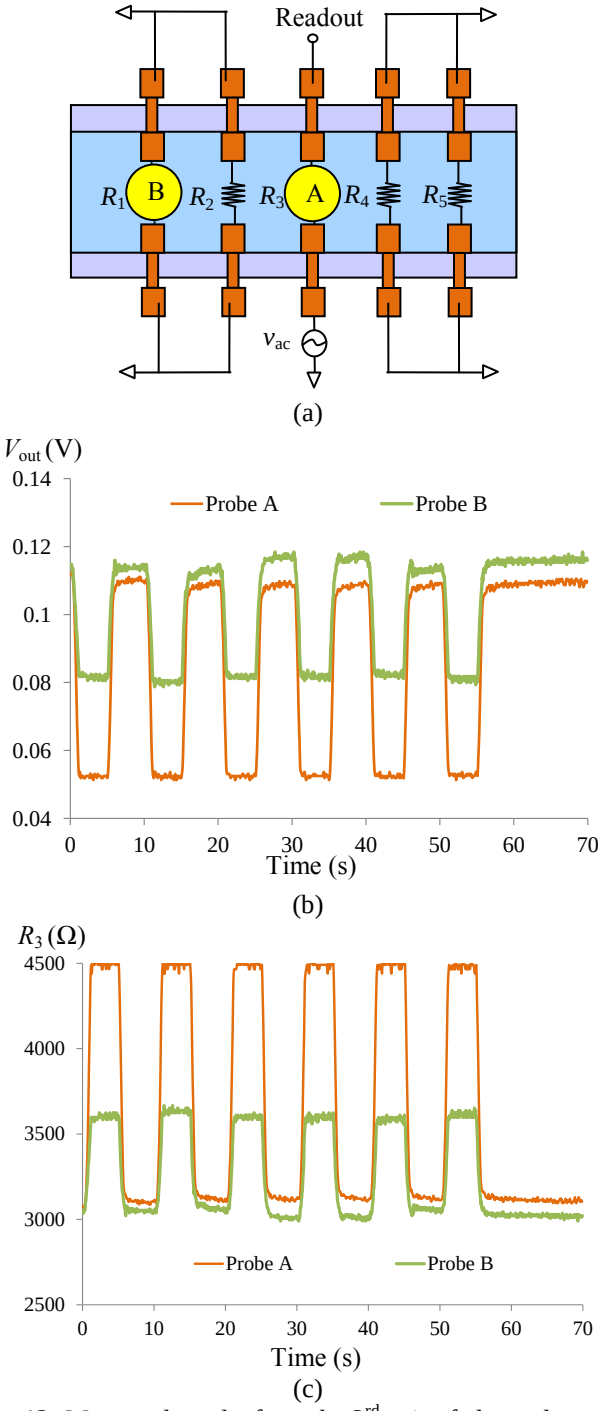

Fig. 12: Measured results from the 3rd pair of electrodes, when the custom probe is located at A and B, respectively (v_{pp}=3V and ω= 200kHz) (a) locations of the probe (b) DC voltage output, and (c) calculated resistance from the DC voltage output

When this sensor is free of external loading, the resistance across this electrode pair is about 3040Ω from the DC output of 0.17V. When this sensor is deflected by 300μm at A, the DC output becomes 0.052V and thus the resistance increases to 4500Ω. The increase in resistance is caused by the cross section reduction of the electrolyte across this electrode pair. Similarly, when the sensor is deflected by 300μm at B, the DC output decreases to 0.082V and the resistance increases to 3600Ω. Since deflecting A causes more reduction in the cross section across the electrode pair than deflecting B, the calculated resistance from deflecting A is higher than that from deflecting B.

The measurement from the 1st and 3rd pairs of electrode validates that this sensor is capable of detecting distributed loads. Ideally, the values of the resistors across all the pairs of electrodes are expected to be very similar, if not exactly the same. The difference in resistance between the 1st and 3rd electrode pairs is believed to be caused by electrolysis on the 3rd electrode pair as a result of high ac voltage (See Fig. 13). A lower ac voltage is expected to avoid such problems.

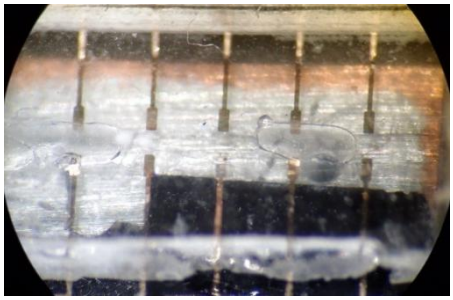

Fig. 13: A picture of the fabricated sensor showing electrolysis on the 3rd electrode pair and an air bubble across the 4th electrode pair

As shown in Fig. 14, when the sensor is free of external loading, the resistance is about 304Ω (one input) when one electrode from the 3rd electrode pair serves as the ac voltage input while all the five electrodes on the other side of the microstructure are connected together and serve as the output. In contrast, when the sensor is free of external loading, the measured resistance is about 730Ω when all the five electrodes on one side of the microstructure are connected together and serve as the ac voltage input while the other five electrodes are connected together and serve as the output. Note that these resistance values are consistent with those obtained in measuring the 1st and 3rd electrode pairs, individually.

Finally, it should be pointed out that, as compared with the pre-defined deflection pattern, the DC output does not exhibit any time delay, proving that the time constant of the sensor itself is below 100ms, since the data is recorded at a time interval of 100ms, while the time constant of the electronic circuit, 12ms, is well below this time interval.

Static performance

To obtain the relation of the resistance to the deflection of this sensor, the circular probe is located at A to deflect the sensor at different deflection levels, and the corresponding DC

voltage output is recorded at each pair of electrodes, respectively. Note that the DC output is recorded from each electrode pair separately, while the probe is kept at A, deflecting the sensor in the same way. Fig. 15(a) shows the recorded DC voltage versus the deflection at A. According to the measured relation of the DC voltage versus the deflection at A, the resistance of each electrode pair is plotted against the deflection at A in Figs. 15(b) and 15(c).

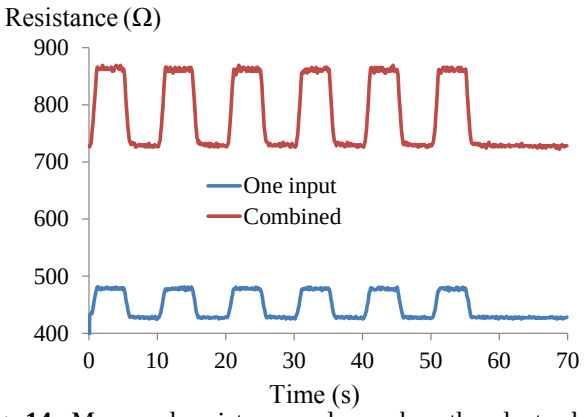

Fig. 14: Measured resistance values when the electrodes are connected together

Since the probe is located right above the top of the 3rd electrode pair, the resistance across this electrode pair changes the most, as evidenced by its slope, 8.1609Ω/μm. The 2nd and 4th pairs are close to the probe and demonstrate slopes of 0.8133Ω/μm and 0.2805Ω/μm, respectively. The 1st and 5th pairs are further away from the probe, and thus demonstrate lower slopes of 0.2165Ω/μm and 0.1491Ω/μm, respectively. The relatively high resistance of the 5th electrode pair is due to the existence of an air bubble during the measurement. It should be noted that after all the measurements were finished, the air bubble has moved to the location across the 4th electrode pair, as shown in Fig. 13. It is believed that misalignment of the probe on the sensor is one of the causes for the large discrepancy on the measured slope of resistance to deflection, because the measurement was conducted on one electrode pair at a time, due to the lack of enough equipment. Another cause for the asymmetry in the measure slopes of the electrode pairs is the existence of the air bubble.

4.4 Discussion

The maximum deflection of the probe used in the measurement is 300μm, while the height of the microchannel is 200μm. From the 3rd electrode pair in Fig. 15(b), at the beginning, the probe is not in full contact with the sensor surface, since the resistance remains flat for the deflection of a few microns. The resistance becomes flat again, indicating that the top of the PDMS microstructure has touched the bottom of the microchannel shortly after the deflection passes 250μm. Therefore, the rest of the 300μm deflection is caused by the deformation of the top of PDMS microstructure.

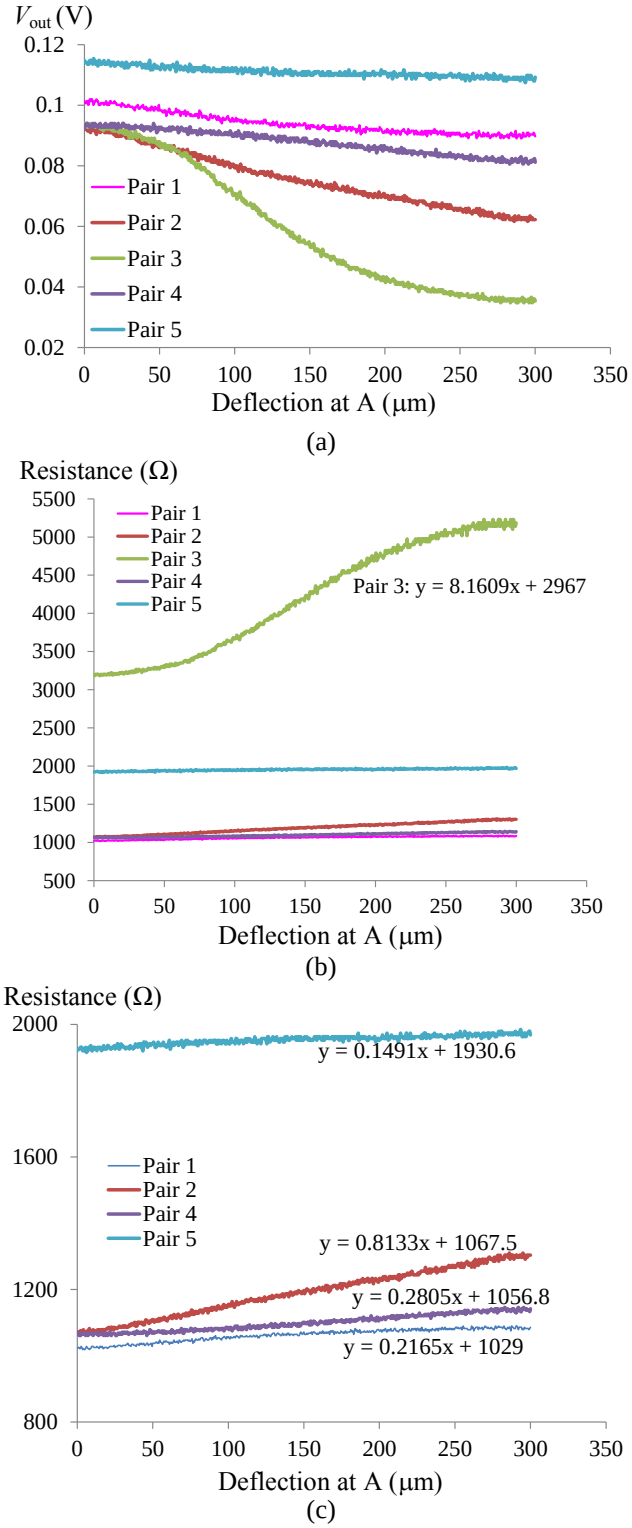

Fig. 15: Measured results from all the five pairs of electrodes, when the custom probe is located at A (a) DC voltage output versus the deflection at A (b) the slope of the calculated resistance versus the deflection at A for the 3rd electrode pair, and (c) the slopes of the calculated resistance versus the deflection at A for the other four electrode pairs

Since this device is aimed to measure distributed loads by monitoring resistance changes across five electrode pairs, it is necessary to characterize the initial electrical resistance of

each individual electrode pair. This can be achieved by separately measuring the resistance from each electrode pair without any external loads. Due to the fact that the five resistors are realized using one electrolyte fluid, the coupling between the five resistors exists in each measured resistance. Therefore, the measured resistances need to be analyzed for obtaining the initial resistance of each electrode pair.

Owing to the lack of a force/pressure sensor, no force is directly recorded in all the measurements. Therefore, the force experienced by the sensor when the probe deflects the sensor is obtained by resorting to finite element modeling. To predict the relation of the deflection of the PDMS rectangular microstructure to distributed loads, a nonlinear finite element model is created in COMSOL software. Since a circular probe of 4mm in diameter is utilized to deflect the sensor at different locations to mimic distributed loads. Therefore, the loading condition applied to the sensor in the model is different deflection levels at different locations along the microstructure length. The simulation results yield the force acting on the device from the deflection of the circular probe. Electrolyte in the microchannel is not expected to affect the deflection-force relation of the device. Thus, only the PDMS rectangular microstructure is modeled. The material properties of PDMS used in the model are listed in Table 2.

Table 2 Key design parameters of the PDMS-based microfluidic resistive tactile sensors

Property	**Value**
Young's modulus, E (kPa)	700
Poisson's ratio, υ	0.45
Density, ρ (kg/m^3)	1000

Fig. 16 shows the deformation in the PDMS microstructure under a deflection of 100μm of the circular probe located at the top of the 3rd pair of electrodes. The simulation gives rise to a force of 1.01N.

Fig. 17 shows the simulated deflection profile of the bottom central line along the microstructure length, in response to different deflection levels of the circular probe located at A. The deflection profile of the top central line along the microstructure length under a deflection of 100μm is also shown in the figure. From this figure, it is clear that a force acting on the center of the device has a much larger effect on the deflection across the neighboring pairs of electrodes than the pairs at the far ends.

6 CONCLUSION

In this paper, we have successfully demonstrated a polymer-based microfluidic resistive sensor for detecting distributed loads, which mimics the scenarios of heterogeneous biological tissues in biomedical applications, viscoelastic materials in manufacturing and food processing applications, and texture of an object in robotics applications. The simple sensor design enables ease of sensor fabrication. Selection of PDMS as the structure material eliminates the need for protective packaging. Complete sealing of electrolyte allows the sensor operating in either aqueous or dry environments. A prototype sensor is fabricated. With a custom built electronic circuit and a custom LabVIEW program, the static and dynamic performance of the fabricated sensor is characterized, demonstrating the design concept of this sensor. Future work will focus on fabricating the sensor using standard photolithography and conducting a scaling analysis for establishing its performance limit and tailoring the sensor design for different applications.

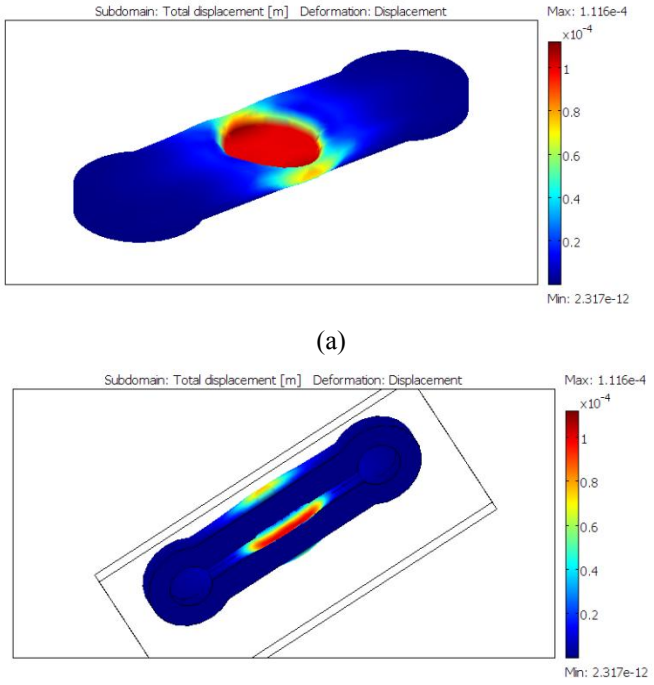

Fig. 16: Simulated deformation of the PDMS rectangular microstructure in response to a deflection of 100μm of a 4mm-in-diameter circular probe located at the top of the 3rd electrode pair (a) top view and (b) bottom view

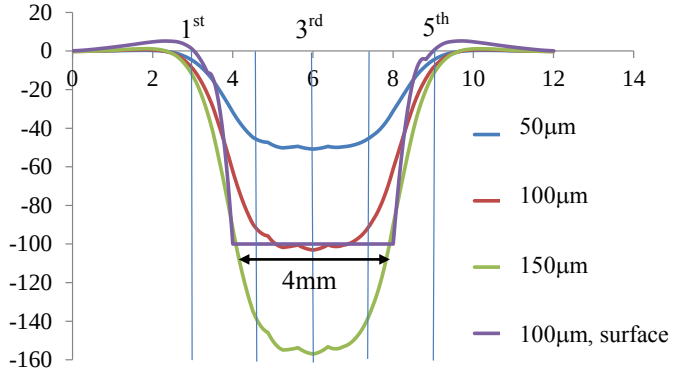

Fig. 17: Simulated deflection profile of the central line along the microchannel length, in response to different deflection levels of the circular probe located at the middle of the device.

7 REFERENCES

[1] Neethirajan, S., Kobayashi, I., Nakajima, M., Wu, D., Nandagopal, S., and Lin, F., 2011, "Microfluidics for food, agriculture and biosystems industries," *Lab on a Chip*, 11, pp.1574-1586.

[2] Liu, C., 2007, "Recent Developments in Polymer MEMS," *Advanced Materials*, 19, pp.3783-3790.

[3] Ahmadi, R., Packirisamy, M., Dargahi, J., and Cecere, R., 2012, "Discretely loaded beam-type optical fiber tactile sensor for tissue manipulation and palpation in minimally invasive robotic surgery," *IEEE Sensor Journal*, 12(1), pp.22-32.

[4] Muhammad, H. B., Oddo, C. M., Beccai, L., Recchiuto, C., Anthony, C. J., Adams, M. J., Carrozza, M. C., Hukins, D. W. L., and Ward, M. C. L., 2011, "Development of a bioinspired MEMS based capacitive tactile sensor for a robotic finger," *Sensors and Actuators A*, 165, pp.221–229.

[5] Hohne, D. H., Younger, J. G., and Solomon, M. J., 2009, "Flexible microfluidic device for mechanical property characterization of soft viscoelastic solids such as bacterial biofilms," *Langmuir*, 25, pp.7743-7751.

[6] Yousef. H., Boukallel. M., and Althoefer. K., 2011, "Tactile sensing for dexertous in-hand manipulation in robotics – a review," *Sensors and Actuators A*, 167(2), pp.171-187.

[7] Puangmali, P., Althoefer, K., Seneviratene, L. D., Murphy, D., and Dasgupta, P., 2008, "State-of-the-art in force and tactile sensing for minimally invasive surgery," *IEEE Sens. J.*, 8(4), pp.371–381.

[8] Dobrzyska, J. A., and Gijs, M. A. M., 2012, "Flexible polyimide-based force sensor," *Sensors and Actuators A*, 173, pp.127–135.

[9] Lee, H. K., Chung, J., Chang, S. I., and Yoon, E., 2011, "Real-time measurement of the three-axis contact force distribution using a flexible capacitive polymer tactile sensor," *J. Micromech. Microeng.*, 21, 035010.

[10] Lu, M., Xiong, J., and Cui, T., 2011, "A flexible tri-axis contact force sensor for tubular medical device applications," *J. Micromech. Microeng.*, 21, 035004.

[11] Gutierrez, C. A. and Meng, E., 2011, "Impedance-Based Force Transduction within Fluid-Filled Parylene Microstructures," *J. Micromech. Microeng.*, 20, pp.1098-1108.

[12] Tseng, W-Y., Fisher, J. S., Prieto, J. L., Rinaldi, K., Alapati, G., and Lee, A. P., 2009, "A slow-adapting microfluidic-based tactile sensor," *J. Micromech. Microeng.*, 19, 085002.

[13] Park, Y-L., Majidi, C., Kramer, R., Berard, P., and Wood, R. J., 2010, "Hyperelastic pressure sensing with a liquid-embedded elastomer," *J. Micromech. Microeng.*, 20, 125029.